PHYSICAL REVIEW B VOLUME 28, NUMBER 2 15 JULY 1983

Extended x-ray-absorption fine structure of Ag impurity atoms in electron-irradiated aluminum

W. Weber and J. Peisl
Sektion Physik der Ludwig-Maximilians Universität München, D-8000 München 22, West Germany
(Received 1 June 1982; revised manuscript received 15 November 1982)

Extended x-ray-absorption fine-structure measurements were used to study radiation-induced defects for 400-ppm Ag impurity atoms in Al samples after irradiation with 2.8-MeV electrons at 95 K and after subsequent thermal-annealing treatment. During irradiation, Al interstitials are mobile and annihilate with vacancies or are trapped by the Ag impurity atoms. After irradiation about $\frac{1}{3}$ of the Ag atoms have captured an Al interstitial atom. A very pronounced new Ag-Al distance $R=2.35$ Å is then observed which can be attributed to the Ag-Al distance in a mixed dumbbell that is formed. The observed distances suggest a $\langle 111 \rangle$ orientation of the mixed dumbbell. During thermal annealing this new structure disappears at about 165 K, and another structure grows at 165 K and disappears at 185 K.

I. INTRODUCTION

The interaction of point defects with impurity atoms plays an important role in the stabilization of radiation-induced defects.[1,2] In pure Al electron irradiation at low temperature produces randomly distributed vacancies and interstitials (Frenkel pairs), which may undergo thermally activated migration and anneal in well-defined annealing stages I (interstitials) and III (vacancies).[3–6] Trapping of interstitials (vacancies) at impurities or cluster formation may stabilize the defects so that they become mobile only at higher temperatures in the annealing stage II (stage IV).

The most direct information on impurity-defect interaction can be obtained from techniques which use the impurity itself as a probe. This is the case for a Mössbauer nucleus [e.g., ^{57}Co in Al (Ref. 7)], and Mössbauer spectroscopy gives information about the neighborhood of the ^{57}Co nucleus via isomer shift and/or quadrupole splittings. In a similar way, perturbed angular correlation measurements of γ rays emitted from a radioactive impurity[8] give information on the change of the electric field gradient by the defects. Both methods, however, are limited to a few favorable isotopes, and the physical information depends on model calculations of the local field changes.

Direct structural information on the surroundings of an impurity can be obtained from extended x-ray-absorption fine-structure (EXAFS) measurements, since they give information on the local environment of the absorbing atom. EXAFS can be a valuable additional probe to study the local structure of an impurity-defect complex on a microscopic scale. It is hoped that EXAFS can be developed as a technique to supplement the above-mentioned microscopic probes. EXAFS measurements are not limited to certain isotopes and can be used for most elements in condensed matter. In the following we report measurements in which the EXAFS technique has been applied, for the first time, to study irradiation-induced defects.[9] In this pioneering experiment, we have selected Ag in Al for several reasons. Ag is known to trap interstitials in Al, and some information about this system is already available from electrical resistivity[10–13] and channeling experiments.[14–16] The large difference in the nuclear charge Z between Ag and Al gives an optimum EXAFS signal-to-noise ratio. When studying the Ag K edge absorption, the Al absorption is very low. Using synchrotron radiation as an x-ray source gives high signal levels but limits the maximum Z of the impurity which can be studied.

In Sec. II we briefly describe the principles of EXAFS and then give some details on the experimental procedures and data processing. The results are presented in Sec. V and are discussed in Sec. VI.

II. PRINCIPLES OF EXAFS

The EXAFS technique allows determination of the local structure around an absorbing atom in condensed matter.[17] The structural information is contained in the EXAFS interference function $\chi(k)$, the normalized oscillatory part of the x-ray-absorption coefficient μ,

$$\chi(k)=\frac{\mu-\mu_0}{\mu_0}=\sum_j N_j\frac{F_j(k)}{2kR_j}\sin[2kR_j+\psi(k)] \times e^{-\sigma_j^2k^2}e^{-\gamma R_j}\,. \quad (1)$$

μ_0 is the smooth, nonoscillating part of the x-ray-absorption coefficient. N_j is the number of atoms in a coordination shell j at a distance R_j. k is the wave vector of the photoelectron. $F_j(k)$ is the backscattering amplitude and $\psi(k)$ the total phase shift, including a phase shift from the absorbing and from the backscattering atom. σ_j^2 is the mean-square fluctuation of the interatomic distance R_j, and γ is a damping factor which accounts for the finite lifetime of the photoelectron final state. In Eq. (1) multiple scattering is not included. In the present experiment it can be neglected since only scattering from first and second neighbors is considered.

III. EXPERIMENTAL PROCEDURES

EXAFS from the impurity element gives information on the sum of all impurity-defect complexes present in the sample. As it is difficult to separate the various contributions, the concentrations of impurities and radiation-induced defects were chosen to yield well-defined impurity-defect complexes. First, the Ag concentration in Al was kept low such that mainly single impurities were present. The typical impurity concentration was about 400 ppm. This is far below the solubility limit for Ag in Al.[18] Assuming a random Ag distribution on substitutional sites, the concentration of Ag pairs or higher agglomerates is expected to be less than 1 ppm. If atoms on second-nearest-neighbor sites are also counted as pairs, this number may at most double. More distant pairs cannot be observed in this experiment and therefore are not considered.

During electron irradiation single interstitial-vacancy pairs are formed. The interstitials are mobile at the irradiation temperature and recombine with vacancies or are trapped at impurities. In order to have mainly single interstitials trapped at Ag impurities, the irradiation dose was such that $C_{\rm int}=130$ ppm, i.e., only one-third of the impurities has trapped an Al interstitial. In order to estimate the probabilities $p(n)$ for an impurity having trapped n interstitials, a Poisson distribution was assumed, following similar considerations by Mansel *et al.*[7] for Co in Al,

$$p(n)=\frac{\bar{n}^n e^{-\bar{n}}}{n}\,. \quad (2)$$

n is the number of self-interstitials trapped at one Ag atom, and $\bar{n}$ is the average ratio of interstitials to impurities $\bar{n}=C_{\rm int}/C_{\rm imp}$. For $\bar{n}\approx\frac{1}{3}$, $p(1)\approx 6p(2)\approx 54p(3)$. Since the contribution of impurities which have trapped two interstitials is hardly detectable in this experiment, the EXAFS spectra consist essentially of two contributions. One comes from isolated Ag impurities on substitutional sites, and the other comes from the irradiation-induced defect structure in which a Ag atom has trapped an Al interstitial. The first structure does not change during irradiation and thermal annealing, whereas the second one is created upon irradiation and should disappear during thermal annealing. Thus the two structures can be easily separated.

Samples were prepared from 99.9999%-pure Al and 99.999%-pure Ag in a high-frequency (HF) vacuum furnace. After etching, the samples were cold rolled to a thickness of about 1 mm. This thickness was a compromise between a thin sample necessary for creating a homogeneous defect distribution from electron irradiation and the optimum thickness $d=2.6/\mu_t=4$ mm (μ_t is the total x-ray-absorption coefficient) for an x-ray-absorption experiment. The samples were cut to a proper shape and, after another etching, homogenized at 580 °C for 24 h in air and slowly cooled to room temperature. The actual Ag concentration of the final sample was determined by neutron activation analysis to be $C_{\rm imp}=400\pm5$ ppm. The samples, clamped in vacuum to a liquid-nitrogen–cooled finger were irradiated by 2.8-MeV/20 μA electrons. The temperature during irradiation was always below 95 K as measured by thermocouples. Simultaneously, a 0.1-mm-thick foil prepared from the same material was irradiated and its electrical resisitivity measured in order to determine the defect concentration. A value of $\Delta\rho_F^T=480$ $\mu\Omega$ cm (Refs. 10 and 19) was used for the resistivity change per unit concentration of trapped Frenkel pairs. Irradiation doses were used so that the trapped Frenkel defect concentration was 130 ± 15 ppm.

The irradiated samples were transferred into a liquid-nitrogen Dewar and transported to Hamburg for the experiment. The EXAFS measurements were performed at the EXAFS setup of the European Molecular Biology Laboratory outstation at DESY, Hamburg. It uses synchrotron radiation from the positrons stored in DORIS. It was operated at 4.5 GeV with a typical current in the 10-mA range. The monochromator consisted of two separately mounted Si (220) single crystals. A slight deviation from the exact parallel arrangement allowed rejection of higher harmonics.[20,21] An ionization chamber filled with Kr and He was used to monitor the primary intensity after the monochromator. The sample could be transferred into the measuring cryostate at liquid-nitrogen temperature without warming up. Measurements were always

performed at 77 K. Intermediate annealing was done for 5-min periods at each given temperature. The experiment was done in the fluorescence mode with a NaI scintillation detector. The sample was positioned at 45° with respect to the incoming beam, and the detector was at 90°. Owing to the polarization of the synchrotron radiation beam, this arrangement reduced Compton scattering background. Measurement control and data collection were performed by a PDP 11 computer.

IV. DATA PROCESSING

The data evaluation for EXAFS experiments has been described by Lee *et al.*[17] We closely followed this procedure, using a computer program developed by Kincaid.[22] From the raw data the background was determined by fitting to polynomials. The resulting $\chi(k)$ was then Fourier transformed. The real and imaginary parts of the Fourier transforms were multiplied by a smooth window function, so that the contribution of only one shell could be selected. The backtransformed $\chi_j(k)$ gives an amplitude function $A_j(k)$ and a phase function $\phi_j(k)$, where j is the number of the shell under consideration,

$$\chi_j(k)=A_j(k)\sin\phi_j(k) . \tag{3}$$

For a proper correction of the energy threshold the phase function is

$$\phi_j(k)=2kR_j+\psi(k) . \tag{4}$$

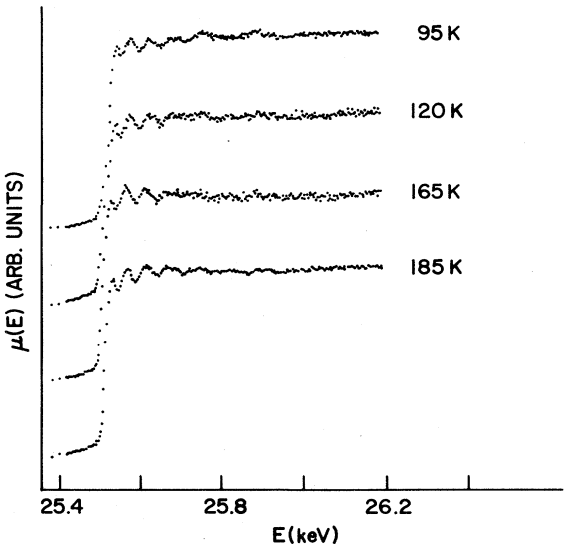

FIG. 1. Absorption coefficient μ of a 400-ppm AgAl alloy vs x-ray energy E close to the Ag K edge. Irradiation with 2.8-MeV electrons at 95 K produced 130-ppm trapped Frenkel pairs. All measurements were at 77 K. Annealing at each temperature was for 5 min.

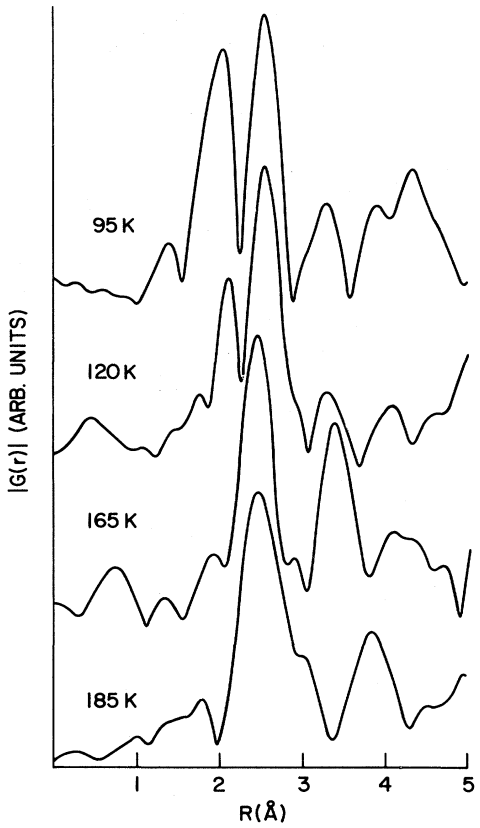

FIG. 2. $|G(r)|$ Fourier transform of the EXAFS interference function $\chi(k)$ obtained from the curves given in Fig. 1.

Theoretical values from Teo and Lee[23] were used for $\psi(k)$, since no suitable model substance was available to determine the AgAl phase function experimentally. The desired R_j were thus obtained.

V. RESULTS

Typical $\mu(E)$ EXAFS curves are shown in Fig. 1. The absorption coefficient μ in arbitrary units is plotted versus x-ray energy for a sample after irradiation (95 K) and after subsequent thermal annealing treatments at the indicated temperatures. Figure 2 shows the Fourier tranforms of $\chi(k)$ for the data given in Fig. 1.

Table I gives results for the radial distances R_j to the Ag neighbors. Of the four observed distances given in Fig. 2 and Table I, two are present in all data sets. First, there is a very strong maximum corresponding to a mean distance of $R_2=2.84\pm0.02$ Å (second row of Table I). It is present in all measurements and shows no systematic shift of its position or amplitude. As it occurs also in an unirradiated sample it cannot be caused by an irradiation-induced effect. The observed value is in close agree-

TABLE I. Distance R_j of Al atoms from the Ag atom after irradiation (95 K) and thermal annealing at the given temperature T. (Numbers in parentheses are less reliable.)

T (K)	R_1 (Å)	R_2 (Å)	R_3 (Å)	R_4 (Å)
95	2.34	2.86	(3.60)	(4.08)
120	2.35	2.85	(3.60)	(4.20)
165		2.83	3.62	(4.29)
185		2.87		4.13
210		2.82		4.10
270		2.82		4.15

ment with the nearest-neighbor distance in pure Al, which is $R_2=2.85$ Å. Indeed, we must expect to observe this agreement since from measured lattice parameter changes upon Ag admixture in Al one can calculate that this distance may increase at most by 0.01 Å due to the slightly larger size of the Ag atom.[24] To a very good approximation the nearest-neighbor distance is the same in pure Al and in $Al_{1-x}Ag_x$. The question arises whether the second fcc nearest-neighbor distance of $R_4=4.03$ Å can be observed, too. We attribute the weak maximum in the data (fourth row in Table I) to this distance, although it is not always clearly distinguished from noise.

The remaining two distances change with irradiation and annealing, so they must be impurity-defect distances. The distance $R_1=2.34$ Å given in the first row of Table I is very pronounced after irradiation at 95 K, becomes smaller after annealing at 120 K, and has disappeared at 165 K. A second defect-related distance $R_3=3.62$ Å is very weak up to 120 K, becomes stronger at 165 K, and has disappeared at 185 K (third row of Table I). This second defect-related structure grows when the first defect structure vanishes. Whether this is due to a change of the defect structure or defect reaction cannot be decided so far.

VI. DISCUSSION

The observed distances will now be compared with some reasonable models for the impurity-defect complex. The first defect-related distance $R_1=2.35$ Å can be well explained as being due to a mixed dumbbell formed by a Ag atom and an Al interstitial on one lattice site. It is quite plausible that the Ag-Al distance for such a dumbbell is smaller than the nearest-neighbor distance in the lattice. The orientation of the dumbbell in the lattice cannot be determined directly. The number and magnitude of the additionally expected distances depend, however, on the orientation of the dumbbell.

The structure of the interstitial in electron-irradiated pure Al has been investigated by diffuse x-ray scattering.[19,24] Here dumbbells are formed in ⟨100⟩ orientation. The distance between the two dumbbell atoms is 2.42 ± 0.2 Å, and the nearest neighbors of the dumbbell are shifted outwards by $0.1a_0$ (a_0 is the lattice parameter). This shift can be assumed to be the same for all 12 neighbors of a dumbbell as the distortion field has almost cubic symmetry.[19]

If we assume that the lattice distortions around a mixed dumbbell are not much different from those in pure Al and that in a mixed dumbbell the Al and the Ag atom have the same distance from the lattice site, then a ⟨100⟩ orientation of the dumbbell is not consistent with the EXAFS data. One would expect another pronounced distance of $R=2.56$ Å which is not observed.

For the ⟨111⟩ orientation, however, we expect within the accessible range no additional maxima, which is in accordance with the experimental findings. Similar considerations for the ⟨110⟩-oriented dumbbell are much more complicated, but one would expect for this case much shorter distances, which are actually not observed.

Quite different models are possible and might also give reasonable results. Further investigation of this problem is necessary to determine the orientation of the mixed Al-Ag dumbbell.

An annealing behavior from the EXAFS results is compared in Fig. 3 with other results from the literature. The remaining percentage of the property change under consideration is plotted versus annealing temperature. The temperature range where a

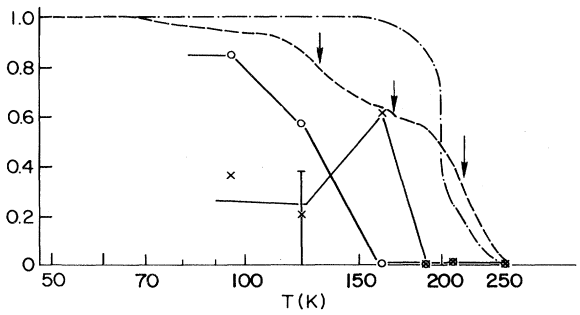

FIG. 3. Annealing behavior of electron-irradiated dilute AgAl alloys. Each property change is normalized to its value after irradiation. ○, ×, EXAFS structure, 400-ppm Ag, 130-ppm Frenkel defects by 1.4×10^{19}/cm^2 electron irradiation; ——, lines joining data points, to guide the eye; — — —, electrical resistivity change (Ref. 10) 50-ppm Ag, 25-ppm Frenkel defects by electron irradiation; —·—·—·, displacement fraction observed in a channeling experiment (Ref. 14), 800-ppm Ag, defects produced by He-ion bombardment.

strong recovery of the EXAFS changes occurs is in good agreement with the partial annealing of the electrical resistivity change in a more dilute electron-irradiated AgAl alloy[10,11] in this temperature range. It disagrees, however, with the annealing behavior after He-ion irradiation reported[14–16] by Swanson and Howe, who observed a strong annealing only around 200 K. They also favor a ⟨100⟩ dumbbell structure.

The present EXAFS data show no annealing around 200 K. The corresponding Al-Ag distance therefore must be larger than about 4 Å and thus merge into the noise or accidentally coincide with the strong maximum R_2 in Table I, which has been identified with a lattice distance and is unchanged with annealing temperature.

ACKNOWLEDGMENTS

We thank B. M. Kincaid for kindly supplying his computer program for data evaluation and G. Materlik, J. Bordas, and J. Philipps for their assistance during the experiments at DESY. Thanks are due to G. Hietel and co-workers of the Gesellschaft für Strahlen- und Umweltforschung, Neuherberg, for their assistance with the electron irradiation, as well as to H. Stärk from the Institut für Radiochemie of the Technische Universität München for the neutron activation analysis of the samples. We thank G. S. Cargill III for critically reading and a revision of the manuscript in English. This work was supported by the Bundesministerium für Forschung und Technologie.

[1]H. Wollenberger, J. Nucl. Mat. 69&70, 362 (1978).
[2]K. Robrock, L. Rehn, V. Spiric, and W. Schilling, Phys. Rev. B 15, 680 (1977).
[3]W. Schilling, P. Ehrhard, and K. Sonnenberg, in Conf. No. 751006-P1 (U.S. GPO, Washington D.C., 1975), p. 470.
[4]A. Seeger, in Ref. 3, p. 493.
[5]F. W. Young, Jr., Nucl. Mater. 69-70, 310 (1978).
[6]R. W. Balluffi, J. Nucl. Mater. 69-70, 240 (1978).
[7]W. Mansel, M. Meyer, and G. Vogl, Radiat. Eff. 35, 69 (1978).
[8]E. Recknagel and T. Wichert, Nucl. Instrum. Methods 182-183, 439 (1981).
[9]Preliminary results have been reported by W. Weber and J. Peisl, in *Proceedings of the Yamada Conference V on Point Defects and Defect Interactions in Metals,* edited by J.-I. Takamura, M. Doyama, and Mokiritani (University of Tokyo Press, Tokyo, 1981), p. 368.
[10]F. Dworschak, R. Lennartz, T. Monsau, and H. Wollenberger, in Ref. 3, p. 601.
[11]F. Dworschak, T. Monsau, and H. Wollenberger, J. Phys. F 6, 2207 (1976).
[12]R. Rizk, P. Vajda, F. Maury, A. Lucasson, P. Lucasson, C. Dimitrov, and O. Dimitrov, J. Appl. Phys. 47, 4740 (1976).
[13]H. Wollenberger, J. Nucl. Mater. 69-70, 362 (1978).
[14]M. L. Swanson and F. Maury, Can. J. Phys. 53, 117 (1975).
[15]M. L. Swanson, L. M. Howe, and A. F. Quenneville, J. Phys. F 6, 1629 (1976).
[16]M. L. Swanson, L. M. Howe, and A. F. Quenneville, J. Nucl. Mater. 69-70, 372 (1978).
[17]P. A. Lee, P. H. Citrin, P. Eisenberger, and B. M. Kincaid, Rev. Mod. Phys. 53, 769 (1981).
[18]M. Hansen, *Constitution of Binary Alloys* (McGraw-Hill, New York, 1958).
[19]P. Ehrhart, J. Nucl. Mater. 69, 200 (1978).
[20]M. Hart and A. R. Rodrigues, J. Appl. Crystallogr. 11, 248 (1978).
[21]J. H. Beaumont and M. Hart, J. Phys. E 7, 823 (1974).
[22]B. M. Kincaid (private communications).
[23]Boon-Keng Teo and P. A. Lee, J. Am. Chem. Soc. 101, 2815 (1979).
[24]H. G. Haubold, Berichte der Kernforschungsanlage Jülich, No. Jül-1090-F, 1974 (unpublished).